PLOS ONE

Intracellular Cleavage of Amyloid β by a Viral Protease NIa Prevents Amyloid β-Mediated Cytotoxicity

Baehyun Shin[1,3], Hyejin Oh[2,3], Sang Min Park[1], Hye-Eun Han[1], Michael Ye[1], Woo Keun Song[2], Woo Jin Park[1]*

1 School of Life Sciences, Gwangju Institute of Science and Technology, Gwangju, Korea, 2 Bio Imaging and Cell Dynamics Research Center, School of Life Sciences, Gwangju Institute of Science and Technology, Gwangju, Korea, 3 Center for Human Genetic Research, Massachusetts General Hospital, Boston, Massachusetts, United States of America

Abstract

Nuclear inclusion a (NIa) of turnip mosaic virus is a cytosolic protease that cleaves amyloid β (Aβ) when heterologously overexpressed. Lentivirus-mediated expression of NIa in the brains of APP(sw)/PS1 mice significantly reduces cerebral Aβ levels and plaque depositions, and improves behavioral deficits. Here, the effects of NIa and neprilysin (NEP), a well-known Aβ-cleaving protease, on oligomeric Aβ-induced cell death were evaluated. NIa cleaved monomeric and oligomeric Aβ at a similar rate, whereas NEP only cleaved monomeric Aβ. Oligomeric Aβ-induced cytotoxicity and mitochondrial dysfunction were significantly ameliorated by NIa, but not by NEP. Endocytosed fluorescently-labeled Aβ localized to mitochondria, and this was significantly reduced by NIa, but not by NEP. These data suggest that NIa may exerts its protective roles by degrading Aβ and thus preventing mitochondrial deposition of Aβ.

Introduction

Alzheimer's disease (AD) is the most prevalent neurodegenerative disorder that is characterized by progressive memory impairment and cognitive dysfunction. The hallmarks of AD are the formation of intracellular neurofibrillary tangles composed of hyper-phosphorylated tau and extracellular amyloid plaques mainly composed of amyloid β (Aβ). Aβ is generated through sequential cleavage of amyloid precursor protein (APP) by β- and γ-secretases [1,2].

Aβ exists as soluble monomers and oligomers, and insoluble fibrils. Which of these forms of Aβ is the active species that are responsible for synaptic loss and neurodegeneration in AD is controversial [3,4]. Neither monomeric nor fibrillar forms of Aβ appear to be responsible [4,5]. Rather, a number of studies indicate that oligomeric Aβ is the most potent neurotoxic species in association with AD [6,7,8,9,10]. For example, oligomeric Aβ reduces neuronal viability approximately 10-fold more efficiently than fibrillar Aβ [11].

Aβ levels in healthy brain are delicately regulated by a dynamic equilibrium between production of Aβ from APP and clearance of Aβ via perivascular drainage or enzymatic degradation. The cytotoxic process of AD is closely linked to an imbalance between the production and clearance of Aβ [12]. Therefore, restoration of this balance by increasing the degradation of Aβ might be a valid therapeutic modality for the treatment of AD [13]. Several endogenous proteases can degrade Aβ. Among these, neprilysin (NEP) is considered to be the physiological regulator of the Aβ

levels in the brain parenchyma [14,15,16]. Intracerebral injections of a recombinant lentivirus expressing human NEP reduce Aβ deposits and neurodegenerative alterations in a mouse model of amyloidosis [17]. Implantation of primary fibroblast cells that express a secreted form of human NEP also significantly reduces plaque burdens in the mouse brain [18]. Consistently, the genetic ablation of NEP in mice markedly increases Aβ levels in whole brain and plasma, increases plaque burdens in the hippocampus, and leads to the development of AD-like neuropathology [19]. Lentivirus-mediated long-term expression of NEP improves behavioral performances and ameliorates neurodegenerative pathology in APP mice [20]. However, the therapeutic potential of NEP is controversial as over-expression of NEP failed to reduce the toxic oligomeric Aβ levels nor improve cognitive deficits in AD mice although it did reduce plaque formation [21].

Nuclear inclusion a (NIa) of turnip mosaic virus is a cytosolic protease with a strict substrate specificity for the consensus sequence of Val-Xaa-His-Gln [22]. In an *in vitro* study, we demonstrated that NIa specifically cleaves Aβ, which contains the Val-His-His-Gln sequence near to its putative α-secretase cleavage site [23]. We further showed that lentivirus-mediated expression of NIa in the brain of AD mice significantly reduced Aβ pathology and improved behavioral deficits [23,24].

Several lines of evidence have suggested that the progression of AD may be associated with mitochondrial dysfunction [25,26]. Aβ inhibits import of nuclear-encoded mitochondrial proteins, and subsequently impairs mitochondrial functions and morphology [27]. In neurons, the overexpression of Aβ results in mitochondrial

fragmentation and an abnormal subcellular distribution of mitochondria by evoking an imbalance between mitochondrial fusion and fission [28]. Furthermore, Aβ impairs oxidative phosphorylation and ATP production in transgenic AD mice [29].

Here, we compared the functions of NIa and NEP, and found that NIa, but not NEP, cleaved oligomeric Aβ and prevented Aβ-induced cytotoxicity and mitochondrial dysfunction in human neuroblastoma cells. By tracing exogenously added Aβ, we determined that NIa prevents localization of endocytosed Aβ to mitochondria. Our study suggests that disruption of Aβ trafficking to mitochondria via intracellular degradation of Aβ is a valuable approach for preventing Aβ-induced cytotoxicity.

Results

NIa, but not NEP, Cleaves Oligomeric Aβ *In vitro*

We first performed an *in vitro* cleavage assay to compare the proteolytic activities of NIa and NEP for Aβ. Monomeric and oligomeric Aβ were incubated with the same amounts of purified NIa and NEP, and were then analyzed by Western blotting. Cleavage of Aβ was discerned by the disappearance of protein bands corresponding to intact monomeric and oligomeric Aβ. As expected, monomeric Aβ was efficiently cleaved by both NIa and NEP (Figure 1). However, oligomeric Aβ was only cleaved by NIa, not by NEP (Figure 1B). Notably, NIa cleaved both monomeric and oligomeric Aβ indistinguishably with a similar catalytic activity. To the best of our knowledge, NIa is the only cytosolic

protease that can cleave both monomeric and oligomeric Aβ with a strict substrate specificity.

NIa, but not NEP, Prevents Oligomeric Aβ-mediated Cytotoxicity

We next examined whether NIa or NEP can inhibit oligomeric Aβ-mediated cytotoxicity in human neuroblastoma SH-SY5Y cells. The cells were transformed with plasmids expressing HA-tagged NIa or NEP. Expression of NIa and NEP was assessed by Western blotting with an anti-HA antibody (Figure 2A). The amounts of plasmids used for cell transformations were adjusted so that the expression levels of NIa and NEP were almost equal in all the subsequent experiments.

Treatment of SH-SY5Y cells with oligomeric Aβ for 48 h reduced cell viability in a dose-dependent manner (Figure S1). The most prominent effects were seen with 10–20 μM Aβ. Thus, 10 μM oligomeric Aβ was used to observe the cytotoxic effects of Aβ in all the subsequent experiments. Under these conditions, Aβ reduced cell viability by ~35% as assessed by 3-[4,5-dimethylthi-zaol-2-yl]-2,5-diphenyl tetrazolium bromide (MTT) assays (Figure 2B). This effect was significantly inhibited by NIa (~16% reduction vs. control) but not by NEP (Figure 2B). Aβ-mediated cytotoxicity can also be monitored by nuclear fragmentation and condensation, a phenomenon known as pyknosis. Under control conditions, only 1–2% of cells underwent pyknosis as observed using a fluorescence microscope. In line with previous reports [30,31], Aβ increased the percentage of pyknotic cells to ~17%. This Aβ-mediated pyknosis was significantly reduced by
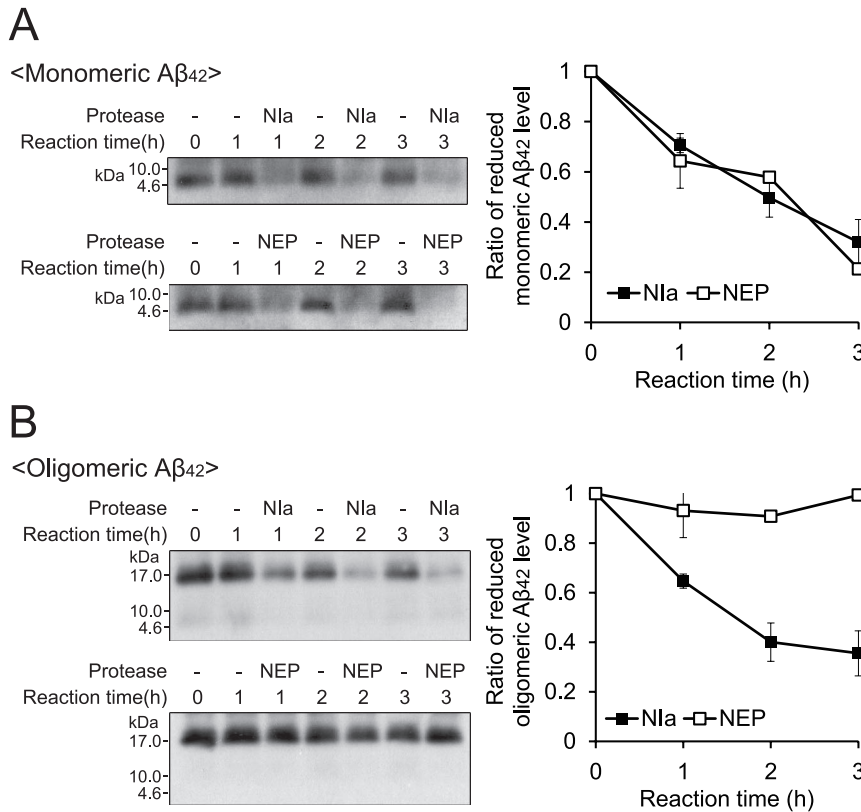
Figure 1. In vitro cleavage of Aβ by NIa and NEP. For the cleavage assay, 2.5 μM of monomeric (**A**) and oligomeric Aβ (**B**) were incubated with 0.5 μM of purified NIa or NEP for 1, 2, and 3 h. The reaction mixture was separated on a PeptiGel (Elpis Biotech), blotted, and probed with the anti-Aβ 6E10 antibody. The densities of the intact Aβ bands were quantified using NIH ImageJ software and plotted. Each data point and error bar represents the mean ± SD (n = 3).
doi:10.1371/journal.pone.0098650.g001
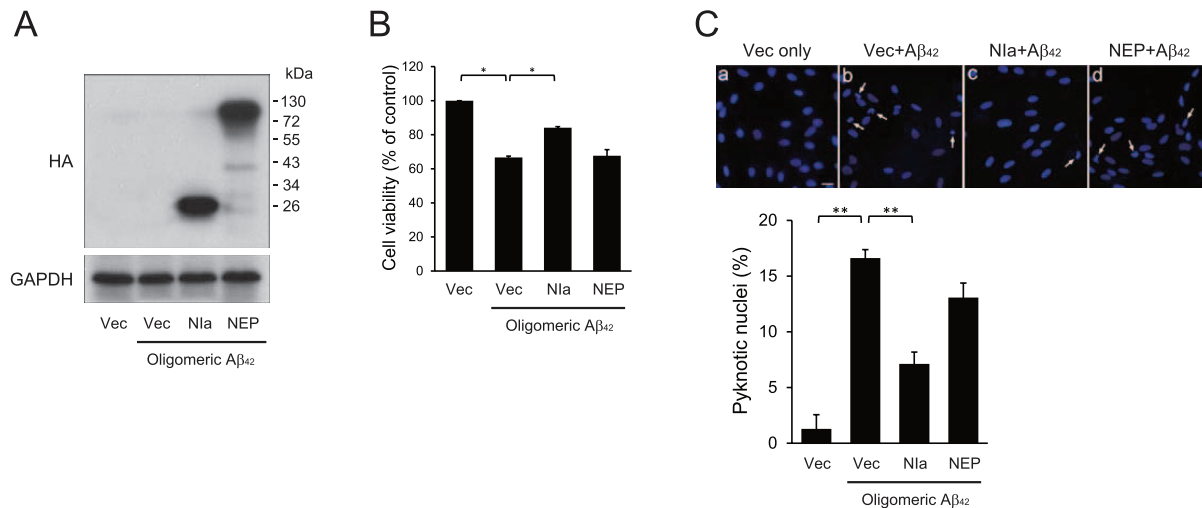
Figure 2. NIa, but not NEP, prevents Aβ-mediated cytotoxicity. Human neuroblastoma SH-SY5Y cells were transfected with pcDNA with no insert (Vec), or with pcDNA with cDNA encoding HA-NIa (NIa) or HA-NEP (NEP). After 24 h of incubation, cells were treated with 10 μM of oligomeric Aβ for an additional 48 h. (**A**) Western blotting with an anti-HA antibody showed that the expression levels of NIa and NEP were similar. GAPDH (detected with an anti-GAPDH antibody) was used as the loading control. (**B**) Cell viability was determined by using the MTT assay. Each bar and error bar represents the mean ± SD (n = 3); *$p < 0.05$. (**C**) Cells were stained with Hoechst 33342 and viewed under a fluorescence microscope. Arrows indicate cells with pyknotic nuclei. The number of pyknotic nuclei was counted and plotted. Scale bar, 50 μm. Each bar and error bar represents the mean ± SD (n = 8); **$p < 0.01$.
doi:10.1371/journal.pone.0098650.g002

NIa (~7%), but not by NEP (Figure 2C). Collectively, these results indicate that NIa, but not NEP, prevents oligomeric Aβ-mediated cytotoxicity.

NIa, but not NEP, Ameliorates Oligomeric Aβ-mediated Mitochondrial Dysfunction

Aβ reportedly is associated with mitochondrial dysfunction [27]. Thus, we examined whether NIa or NEP affect Aβ-induced mitochondrial dysfunction in SH-SY5Y cells. To monitor mitochondrial membrane potential (Ψm) using a confocal microscope, we utilized JC-1, which exists as a green-fluorescent J-monomer at depolarized membrane potentials and as a red-fluorescent J-aggregate at hyperpolarized membrane potentials. A decrease in the ratio of red fluorescence to green fluorescence indicates a decrease in Ψm. As expected, Aβ significantly reduced Ψm, which was reversed by NIa, but not by NEP (Figure 3A).

Next, we utilized the cell-permeable fluorescent dye dihydroethidium (DHE) to monitor the production of reactive oxygen species (ROS). When DHE is oxidized by superoxide anions to oxoethidium, it intercalates into DNA and generates red fluorescence [32]. In line with previous reports [33], Aβ increased the percentage of cells with red fluorescence (~33% vs. ~12% in control), which was significantly attenuated by NIa (~21%), but not by NEP (Figure 3B). Taken together, these data indicate that NIa, but not NEP, ameliorates Aβ-mediated mitochondrial dysfunction.

NIa, but not NEP, Prevents Accumulation of Aβ in Mitochondria

We next sought to elucidate how NIa prevents Aβ-mediated mitochondrial dysfunction. To this end, we traced the intracellular trafficking of exogenously added Aβ in SH-SY5Y cells. Oligomeric Aβ was labeled with Alexa Fluor 488 and was then added to the culture media. After 90 min of incubation (pulse), the culture media was replaced with fresh media not containing Aβ and was then further incubated for 90, 270, and 630 min (chase). The cells

were then fixed and co-stained with LysoTracker and Mito-Tracker. After 90 min of chase, ~10% of LysoTracker, but none of the MitoTracker, co-localized with the Alexa Flour. This suggested that the majority of the exogenously added Aβ was present in endosomes, some was present in lysosomes, and none was present in mitochondria at this stage. However, the percentage of LysoTracker or MitoTracker that co-localized with Alexa fluorescence gradually increased as the duration of the chase increased. After 630 min of chase, ~35% of LysoTracker and ~5% of MitoTracker co-localized with the Alexa Flour (Figure 4). These results are consistent with earlier observations that exogenously added Aβ reaches lysosomes via endocytosis, where a portion of the peptide enters mitochondria; however, the mechanism is unknown.

We next examined whether NIa or NEP affect trafficking of oligomeric Aβ to mitochondria. SH-SY5Y cells transformed with plasmids expressing NIa or NEP were treated with Alexa Flour 488-labeled oligomeric Aβ for 18 h. At this time point, most of the Alexa Flour co-localized with either LysoTracker or MitoTracker. Under normal conditions, ~25% and ~5% of LysoTracker and MitoTracker, respectively, co-localized with the Alexa Flour. Neither NIa nor NEP significantly affected the co-localization of LysoTracker with the Alexa Flour (Figure 5A). However, NIa, but not NEP, significantly reduced the percentage of MitoTracker that co-localized with the Alexa Flour (~1%) (Figure 5B). Co-localization of MitoTracker and the Alexa Flour was further confirmed by 3-dimensional reconstruction of the confocal images (Figure S2, Video S1–4). The Alexa Flour represents intact Aβ after incubation for 18 h, supporting the validity of our experimental approach (Figure S3). Collectively, these data suggest that NIa prevents the accumulation of oligomeric Aβ in mitochondria by proteolytically degrading the peptide in the cytosol.
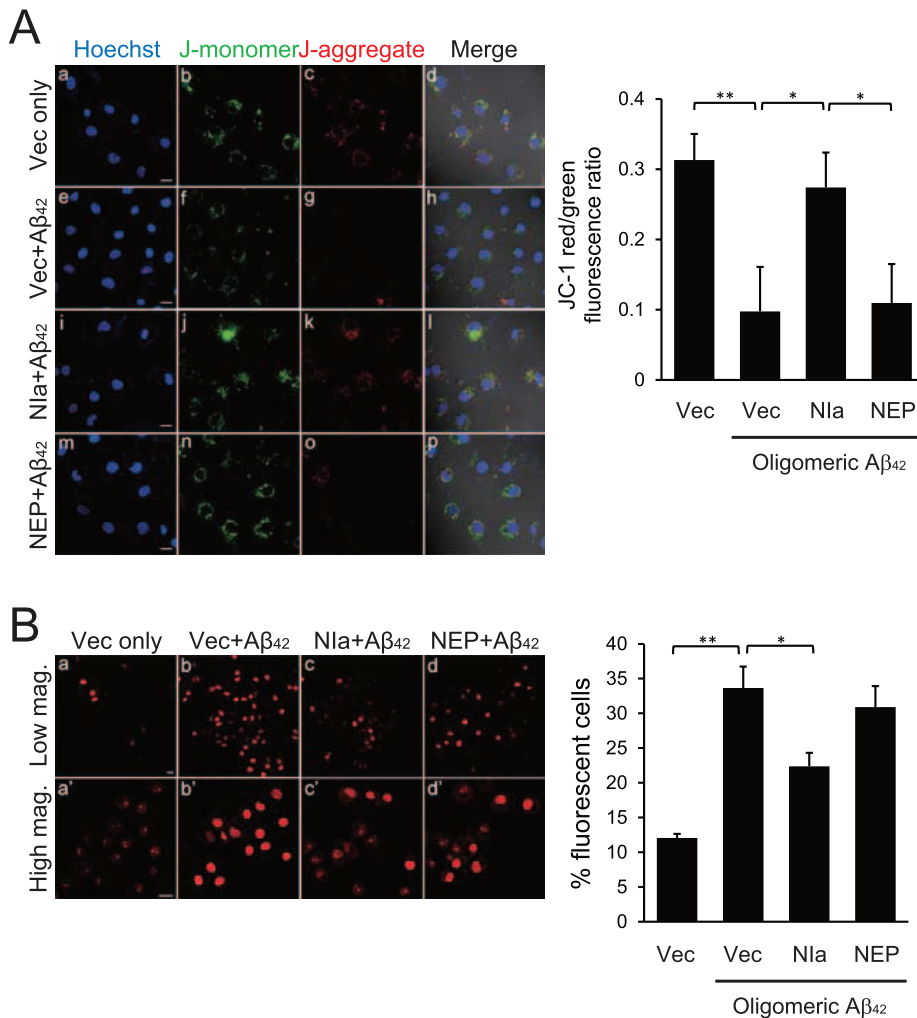
Figure 3. NIa, but not NEP, restores Aβ-mediated mitochondrial dysfunction. Human neuroblastoma SH-SY5Y cells were transfected with pcDNA with no insert (Vec), or with pcDNA with cDNA encoding HA-NIa (NIa) or HA-NEP (NEP). After 24 h of incubation, cells were treated with 10 μM of oligomeric Aβ for an additional 48 h. (**A**) Cells were treated with 2.5 μM of JC-1, an indicator of Ψm, for 15 min at 37°C and visualized by confocal microscopy. The intensities of red and green JC-1 fluorescence were quantitated using the MetaMorph imaging software and their ratios were plotted. Scale bar, 50 μm. Each bar and error bar represents the mean ± SD (n = 7); *$p < 0.05$, **$p < 0.01$. (**B**) Cells were incubated with 30 μM of DHE, an indicator of ROS for 30 min. Low (panels a–d) and high (panels a'–d') magnification images of cells were obtained using a confocal microscope. Data represent the number of fluorescent cells as a percentage of the total number of cells in the observed field. Scale bar, 50 μm. Each bar and error bar represents the mean ± SD (n = 5); *$p < 0.05$, **$p < 0.01$.
doi:10.1371/journal.pone.0098650.g003

Discussion

The NIa protease of turnip mosaic virus has a strict substrate specificity for the consensus sequence of Val-Xaa-His-Gln [22]. This protease is involved in the cleavage of viral polyproteins to generate mature viral proteins. We noticed the same Val-His-His-Gln consensus sequence in Aβ near to its putative α-secretase cleavage site and surmised that this sequence could be cleaved by NIa. Indeed, NIa specifically cleaves Aβ *in vitro* and significantly reduces Aβ-induced cell death in rat neuroblastoma cells [23]. Furthermore, lentivirus-mediated expression of NIa in the brain of AD mice significantly reduces cerebral Aβ levels and plaque depositions, and recovers behavioral deficits [24]. These results raised the possibility that NIa can be used as a therapeutic modality for the treatment of AD.

Currently, more than 20 endogenous Aβ-cleaving enzymes have been identified [34]. Among them, NEP is considered to have a major role in the metabolism of Aβ in the brain. The possible therapeutic use of NEP for AD was proposed because NEP ameliorates neurodegenerative pathology and also improves behavioral performances in APP mice [20]. However, this earlier enthusiasm has been challenged. For examples, over-expression of NEP does not improve cognitive deficits in AD mice [21]. This might be explained, at least partially, because NEP cannot cleave the more toxic oligomeric Aβ, as shown here. In addition, it should be noted that NEP has diverse physiological roles in the brain. For example, overexpression of NEP causes a reduction in cAMP-responsive element-binding protein-mediated transcription, age-dependent axon degeneration, and premature death in flies [35]. Sustained NEP activation may also be detrimental in mammals because NEP can degrade a wide range of circulating peptides, including enkephalin, atrial natriuretic peptide, endothelin, and substance P [36]. Therefore, NIa has certain advantages over NEP as a therapeutic modality for AD with its unique capability of cleaving the more toxic oligomeric Aβ and its relatively high substrate specificity.
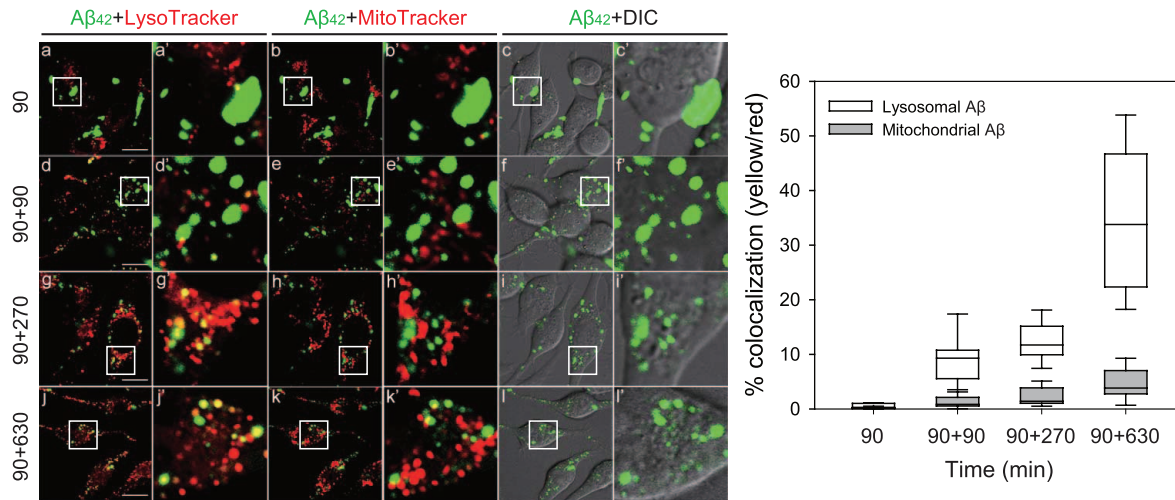
Figure 4. Endocytosed oligomeric Aβ accumulates in lysosomes and mitochondria. Human neuroblastoma SH-SY5Y cells were treated with 2.5 μM of Alexa Fluor-labeled Aβ oligomers for 90 min (pulse) and were further incubated in fresh media for 90, 270, or 630 min (chase). Cells were co-stained with LysoTracker and MitoTracker, and observed under a confocal microscope. The images indicated by the open boxes are shown in a higher magnification in the adjacent columns. The yellow color in the merged image indicates co-localization of green (Alexa Fluor 488-labeled Aβ) and red (LysoTracker, Red/MitoTracker, Deep Red) fluorescence. The percentages of lysosomes (white bars) or mitochondria (gray bars) that co-localized with Aβ were plotted. Scale bar, 50 μm. Each bar and error bar represents the mean ± SD (n = 10). DIC, differential interference contrast.
doi:10.1371/journal.pone.0098650.g004

The controversy surrounding the molecular mechanism underlying the cytotoxicity of Aβ in brains has yet to be settled. Among the several hypotheses, one suggests that Aβ exerts its detrimental effects partly by interfering with mitochondrial functions. Aβ is internalized via raft-mediated endocytosis [37]. The internalized Aβ reaches the mitochondria, where it binds to a mitochondrial enzyme called Aβ-binding alcohol dehydrogenase (ABAD). It remains to be seen how the endocytosed, thus intraluminal, Aβ reaches the mitochondria. The interaction between Aβ and ABAD promotes leakage of ROS, mitochondrial dysfunction, and cell death [38]. Furthermore, inhibition of the Aβ-ABAD interaction using a decoy peptide improves mitochondrial function in AD mice [39]. NIa did not interfere with the internalization of Aβ or with the transport of Aβ to lysosomes, but reduced the amounts of Aβ localized in mitochondria (Figure 5). Therefore, it appears that NIa cleaves Aβ that was in transit from lysosomes to mitochondria. Our chase experiments suggest that Aβ travels through endosomes and lysosomes and that a portion of Aβ further travels to mitochondria (Figure 4). Considering that NIa functions primarily in the cytosol, it is possible that Aβ transiently passes the cytosol during transit from the lysosomes to mitochondria. However, we could not definitively test this hypothesis due to limitations in current imaging techniques. Interpretation of our data is also partially hampered by the fact that the traffic routes allowing the localization of Aβ in mitochondria are largely unknown.

Collectively, we demonstrated that NIa prevents Aβ-mediated cytotoxicity and associated mitochondrial dysfunction by reducing the amounts of Aβ localized in the mitochondria. During the pathogenesis of AD, the route linking lysosomes to mitochondria can be viewed as a "Thermopylae pass". Annihilation of the invading Aβ at this "pass" can be a winning strategy in the battle against AD.

Materials and Methods

Reagents and Materials

Synthetic Aβ42 peptide was purchased from Anygen (Gwangju, Korea). Active recombinant human NEP was from Enzo Life Science International (Farmingdale, NY, USA). Mouse monoclonal anti-Aβ antibody against residues 1–16 (6E10) was purchased from Covance (Princeton, NJ, USA). DHE was from Sigma-Aldrich (St Louis, MO, USA). JC-1, LysoTracker Red DND-99, and MitoTracker Deep Red FM were from Molecular Probes (Eugene, OR, USA). Unless otherwise noted, all other chemicals and reagents were purchased from Sigma.

Preparation of Aβ42 Oligomer

Aβ42 oligomers were prepared according to the method described by Stine et al. [40]. Synthetic Aβ42 peptides were initially solubilized in 1,1,1,3,3,3-hexafluoroisopropanol (Fluka) to a concentration of 1 mM, to monomerize pre-existing aggregates. Following evaporation of the 1,1,1,3,3,3-hexafluoroisopropanol in a fume hood overnight, the resulting peptide film was stored desiccated at −20°C. Subsequently, the peptide was resuspended in anhydrous dimethyl sulfoxide to a concentration of 2.5 mM and bath sonicated for 10 min. To enrich oligomers, phenol-red free Dulbecco's modified Eagle's medium (DMEM; Gibco) was added under continuous vortexing to bring the peptide to a final concentration of 100 μM and incubated at 4°C for 24 h.

Purification of the NIa Protease and *In vitro* Cleavage Assay

Purification of the NIa protease was performed as described by Han et al. [23]. For the *in vitro* cleavage assay, 0.5 μM of purified NIa or recombinant NEP was incubated with 2.5 μM of monomeric or oligomeric Aβ in a time-dependent manner. The buffers used in this reaction were as follows: NIa (20 mM HEPES [pH 7.4], 10 mM KCl, 10 mM MgCl2) and NEP (50 mM Tris-HCl [pH 9.0], 0.05% Brij35). After incubation, the reaction mixture was separated on a PeptiGel (Elpis Biotech), blotted, and probed with the anti-Aβ 6E10 antibody [41].

Cell Culture and DNA Transfection

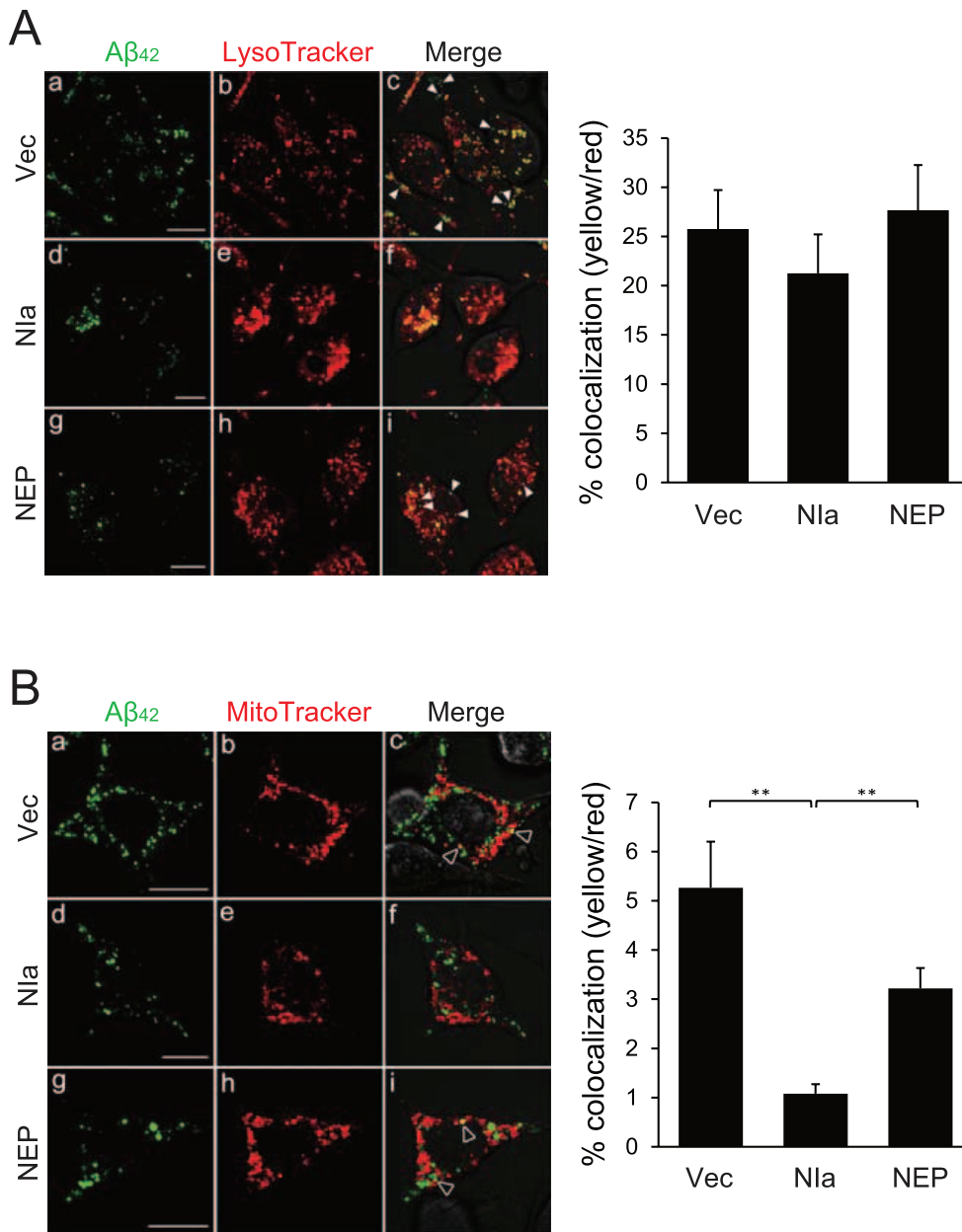Human neuroblastoma SH-SY5Y cells were grown in DMEM (Hyclone) supplemented with 10% fetal bovine serum (Hyclone),

Figure 5. NIa, but not NEP, prevents accumulation of Aβ in mitochondria. Human neuroblastoma SH-SY5Y cells were transfected with pcDNA with no insert (Vec), or with pcDNA with cDNA encoding HA-NIa (NIa) or HA-NEP (NEP). After 24 h of incubation, cells were treated with 2.5 μM of Alexa Fluor 488-labeled Aβ oligomers for an additional 18 h. Cells were stained with LysoTracker (**A**) or MitoTracker (**B**), and observed by confocal microscopy. White arrowheads in panel A indicate Aβ that co-localized with lysosomes and open arrowheads in panel B indicate Aβ that co-localized with mitochondria. The percentages of lysosomes or mitochondria that co-localized with Aβ were plotted. Scale bar, 50 μm. Each bar and error bar represents the mean $\pm$ SD (n = 10); **$p < 0.01$.
doi:10.1371/journal.pone.0098650.g005

100 U/ml penicillin, and 100 μg/ml streptomycin (Invitrogen). Cells were transiently transfected with plasmid DNA using Lipofectamine LTX (Invitrogen) according to the manufacturer's instructions. To express the turnip mosaic virus NIa and the NEP protease in mammalian cells, codon-optimized NIa and NEP genes were subcloned into the pcDNA3 vector (Invitrogen) containing an N-terminal HA tag. A matching vector without an insert was used as a control.

Quantification of Cell Death/Survival

MTT (Sigma) was dissolved in phosphate buffered saline at a concentration of 2.5 mg/ml. A volume of MTT solution equivalent to 20% of the culture media volume was added to the cell culture at 37°C for 2 h. A volume of dimethyl sulfoxide (solubilization solution) equivalent to the culture media volume was added, and cells were placed on a shaker until the resulting formazan crystals were completely dissolved. The absorbance of the samples was measured at 570 nm, and the background absorbance of each well was measured at 690 nm. SH-SY5Y cells were examined for pyknotic nuclei by Hoechst 33342 staining

following the methods described by Wyttenbach *et al.* [42] and Sellamuthu *et al.* [43].

Measurement of Ψm

Ψm was determined by staining SH-SY5Y cells with JC-1 and was measured by confocal microscopy. SH-SY5Y cells were cultured on poly-L-lysine-coated coverslips. After exposure to Aβ, cells were incubated in DMEM containing 2.5 µM JC-1 for 15 min at 37°C. The cells were washed and fluorescent images were then obtained immediately using a Fluoview FV 1000 confocal laser scanning microscope. Data were analyzed with MetaMorph imaging software to quantify the intensities of red and green fluorescence. The results were expressed as the ratio of red fluorescence to green fluorescence.

Measurement of ROS Production

ROS production in SH-SY5Y cells was assayed using the oxidative fluorescent dye DHE. SH-SY5Y cells were cultured on poly-L-lysine-coated coverslips. After exposure to Aβ, cells were loaded with 30 µM of DHE for 30 min at 37°C. The cells were washed to remove excess DHE and fluorescent images were captured immediately using a Fluoview FV 1000 confocal laser scanning microscope. The excitation and emission wavelengths were 510 nm and 590 nm, respectively. Images were analyzed using MetaMorph imaging software. The number of fluorescent cells were counted and represented as a percentage of the total number of cells in each image field.

Labeling of Aβ42 Oligomers

The labeling reaction was performed using the Alexa Fluor 488 Microscale Protein Labeling Kit (Invitrogen). The procedure was described by Jungbauer *et al.* [44] in detail.

Cellular Uptake of Alexa Fluor 488-labeled Aβ42 Oligomers

SH-SY5Y cells were cultured on poly-L-lysine-coated coverslips for 24 h. The cells were treated with 2.5 µM of Alexa Fluor 488-labeled Aβ42 oligomers in phenol-red-free DMEM (Gibco) supplemented with 1% N2 supplement (Invitrogen), 100 U/ml penicillin, and 100 µg/ml streptomycin (Invitrogen) for a further 90 min. At the end of the treatment, cells were further incubated for various lengths of time. Cells grown in the presence of Alexa Fluor 488-labeled Aβ42 oligomers were stained with 200 nM of LysoTracker Red and 100 nM of MitoTracker Deep Red in phenol-red-free DMEM for 30 min at 37°C. The cells were washed extensively and were then visualized immediately using a Fluoview FV 1000 confocal laser scanning microscope equipped with 100× and 60× oil-immersion objectives and capable of additional 3–4× zoom.

Statistical Analysis

Results are expressed as the means ± standard deviation (SD). Comparisons between two groups were performed using the Student's *t*-test. Comparisons between multiple groups were performed by one-way ANOVA with the Bonferroni correction. Statistical analyses were conducted with StatView software version 5.0 (SAS Institute Inc.). A *p*-value of less than 0.05 was considered statistically significant.

Supporting Information

Figure S1 Dose-dependent effects of oligomeric Aβ on cell viability. SH-SY5Y cells were incubated with various concentrations of oligomeric Aβ for 48 h. Cell viability was determined by using the MTT assay. Each bar and error bar represents the mean ± SD (n = 4); **$p<0.01$.
(EPS)

Figure S2 Assessment of mitochondrial accumulation of Aβ by confocal microscopy. SH-SY5Y cells were treated with 2.5 µM of Alexa Fluor-labeled Aβ oligomers for 90 min and were further incubated in fresh media for 630 min. Cells were stained with MitoTracker and observed under a laser scanning confocal microscope. (**A**) Reconstruction of 3-D images was performed with 50–60 Z-directional slices (0.1 µm thick) of the confocal images. The 3-D images were then virtually re-sliced in YZ axis (marked by white broken lines) to obtain transversal images (**a₁, a₂**). Open arrowheads indicate Aβ that co-localized with mitochondria. Note that all the 2 yellow dots seen in XY planes (**a**) are also yellow when observed in YZ planes (**a₁, a₂**). Scale bar, 20 µm. (**B**) The images of the individual Z slices were arranged by their positions along the Z-axis from top to bottom. Arrows in images #6–11 indicate the Aβ fluorescence shown in panel a₁, and arrows in images #19–23 indicate the Aβ fluorescence shown in panel a₂.
(TIF)

Figure S3 Fluorescence of Alexa Fluor-labeled Aβ represents intact Aβ in SH-SY5Y cells. SH-SY5Y cells were treated with 2.5 µM of Alexa Fluor-labeled Aβ (green) for 90 min and were further incubated in fresh media for 18 h. Cells were stained with MitoTracker Red CMXRos (red) and fixed with methanol for 4 min. Aβ was detected either by fluorescence of Alexa Fluor (green) or by immunostaining with the 6E10 antibody (blue). (**A**) Images with low (panels a–e) and high (panels a'–e') magnifications were obtained using a confocal microscope. A filled arrow in merged images indicates Aβ colocalized with MitoTracker, whereas open arrows indicate Aβ not colocalized with MitoTracker. Scale bars, 10 µm. (**B**) Pair-wise merged images were created using the images shown in panel A. Merge 1 shows that all Alexa signals are overlapped with 6E10 signals. Merge 2 and 3 show that one of the Aβ signal is colocalized with MitoTracker. Scale bars, 10 µm.
(PDF)

Video S1 360-degree view of the reconstituted 3-D confocal images. Video was created for the positive dot that was shown in Figure S2 (panel a₁).
(AVI)

Video S2 360-degree view of the reconstituted 3-D confocal images. Video was created for the positive dot that was shown in Figure S2 (panel a₂).
(AVI)

Video S3 360-degree view of the reconstituted 3-D confocal images. Video was created for one of the negative dots that were shown in Figure S2 (panel a).
(AVI)

Video S4 360-degree view of the reconstituted 3-D confocal images. Video was created for one of the negative dots that was shown in Figure S2 (panel a).
(AVI)

Author Contributions

References

1. Shoji M, Golde TE, Ghiso J, Cheung TT, Estus S, et al. (1992) Production of the Alzheimer amyloid beta protein by normal proteolytic processing. Science 258: 126–129.
2. Blennow K, de Leon MJ, Zetterberg H (2006) Alzheimer's disease. Lancet 368: 387–403.
3. Haass C, Steiner H (2001) Protofibrils, the unifying toxic molecule of neurodegenerative disorders? Nat Neurosci 4: 859–860.
4. Klein WL, Krafft GA, Finch CE (2001) Targeting small Abeta oligomers: the solution to an Alzheimer's disease conundrum? Trends Neurosci 24: 219–224.
5. Selkoe DJ (2002) Alzheimer's disease is a synaptic failure. Science 298: 789–791.
6. Lacor PN, Buniel MC, Chang L, Fernandez SJ, Gong Y, et al. (2004) Synaptic targeting by Alzheimer's-related amyloid beta oligomers. J Neurosci 24: 10191–10200.
7. Lesne S, Koh MT, Kotilinek L, Kayed R, Glabe CG, et al. (2006) A specific amyloid-beta protein assembly in the brain impairs memory. Nature 440: 352–357.
8. Townsend M, Shankar GM, Mehta T, Walsh DM, Selkoe DJ (2006) Effects of secreted oligomers of amyloid beta-protein on hippocampal synaptic plasticity: a potent role for trimers. J Physiol 572: 477–492.
9. Shankar GM, Li S, Mehta TH, Garcia-Munoz A, Shepardson NE, et al. (2008) Amyloid-beta protein dimers isolated directly from Alzheimer's brains impair synaptic plasticity and memory. Nat Med 14: 837–842.
10. Villemagne VL, Perez KA, Pike KE, Kok WM, Rowe CC, et al. (2010) Blood-borne amyloid-beta dimer correlates with clinical markers of Alzheimer's disease. J Neurosci 30: 6315–6322.
11. Dahlgren KN, Manelli AM, Stine WB, Jr., Baker LK, Krafft GA, et al. (2002) Oligomeric and fibrillar species of amyloid-beta peptides differentially affect neuronal viability. J Biol Chem 277: 32046–32053.
12. Glabe C (2000) Does Alzheimer disease tilt the scales of amyloid degradation versus accumulation? Nat Med 6: 133–134.
13. Hawkes CA, Hartig W, Kacza J, Schliebs R, Weller RO, et al. (2011) Perivascular drainage of solutes is impaired in the ageing mouse brain and in the presence of cerebral amyloid angiopathy. Acta Neuropathol 121: 431–443.
14. Iwata N, Tsubuki S, Takaki Y, Watanabe K, Sekiguchi M, et al. (2000) Identification of the major Abeta1-42-degrading catabolic pathway in brain parenchyma: suppression leads to biochemical and pathological deposition. Nat Med 6: 143–150.
15. Shirotani K, Tsubuki S, Iwata N, Takaki Y, Harigaya W, et al. (2001) Neprilysin degrades both amyloid beta peptides 1–40 and 1–42 most rapidly and efficiently among thiorphan- and phosphoramidon-sensitive endopeptidases. J Biol Chem 276: 21895–21901.
16. Leissring MA, Farris W, Chang AY, Walsh DM, Wu X, et al. (2003) Enhanced proteolysis of beta-amyloid in APP transgenic mice prevents plaque formation, secondary pathology, and premature death. Neuron 40: 1087–1093.
17. Marr RA, Rockenstein E, Mukherjee A, Kindy MS, Hersh LB, et al. (2003) Neprilysin gene transfer reduces human amyloid pathology in transgenic mice. J Neurosci 23: 1992–1996.
18. Hemming ML, Patterson M, Reske-Nielsen C, Lin L, Isacson O, et al. (2007) Reducing amyloid plaque burden via ex vivo gene delivery of an Abeta-degrading protease: a novel therapeutic approach to Alzheimer disease. PLoS Med 4: e262.
19. Farris W, Schutz SG, Cirrito JR, Shankar GM, Sun X, et al. (2007) Loss of neprilysin function promotes amyloid plaque formation and causes cerebral amyloid angiopathy. Am J Pathol 171: 241–251.
20. Spencer B, Marr RA, Rockenstein E, Crews L, Adame A, et al. (2008) Long-term neprilysin gene transfer is associated with reduced levels of intracellular Abeta and behavioral improvement in APP transgenic mice. BMC Neurosci 9: 109.
21. Meilandt WJ, Cisse M, Ho K, Wu T, Esposito LA, et al. (2009) Neprilysin overexpression inhibits plaque formation but fails to reduce pathogenic Abeta oligomers and associated cognitive deficits in human amyloid precursor protein transgenic mice. J Neurosci 29: 1977–1986.
22. Kang H, Lee YJ, Goo JH, Park WJ (2001) Determination of the substrate specificity of turnip mosaic virus NIa protease using a genetic method. J Gen Virol 82: 3115–3117.
23. Han HE, Sellamuthu S, Shin BH, Lee YJ, Song S, et al. (2010) The nuclear inclusion a (NIa) protease of turnip mosaic virus (TuMV) cleaves amyloid-beta. PLoS One 5: e15645.
24. Kim TK, Han HE, Kim H, Lee JE, Choi D, et al. (2012) Expression of the plant viral protease NIa in the brain of a mouse model of Alzheimer's disease mitigates Abeta pathology and improves cognitive function. Exp Mol Med 44: 740–748.
25. Reddy PH, Beal MF (2008) Amyloid beta, mitochondrial dysfunction and synaptic damage: implications for cognitive decline in aging and Alzheimer's disease. Trends Mol Med 14: 45–53.
26. Pagani L, Eckert A (2011) Amyloid-Beta interaction with mitochondria. Int J Alzheimers Dis 2011: 925050.
27. Sirk D, Zhu Z, Wadia JS, Shulyakova N, Phan N, et al. (2007) Chronic exposure to sub-lethal beta-amyloid (Abeta) inhibits the import of nuclear-encoded proteins to mitochondria in differentiated PC12 cells. J Neurochem 103: 1989–2003.
28. Wang X, Su B, Siedlak SL, Moreira PI, Fujioka H, et al. (2008) Amyloid-beta overproduction causes abnormal mitochondrial dynamics via differential modulation of mitochondrial fission/fusion proteins. Proc Natl Acad Sci U S A 105: 19318–19323.
29. Rhein V, Song X, Wiesner A, Ittner LM, Baysang G, et al. (2009) Amyloid-beta and tau synergistically impair the oxidative phosphorylation system in triple transgenic Alzheimer's disease mice. Proc Natl Acad Sci U S A 106: 20057–20062.
30. Li YP, Bushnell AF, Lee CM, Perlmutter LS, Wong SK (1996) Beta-amyloid induces apoptosis in human-derived neurotypic SH-SY5Y cells. Brain Res 738: 196–204.
31. Magrane J, Christensen RA, Rosen KM, Veereshwarayya V, Querfurth HW (2006) Dissociation of ERK and Akt signaling in endothelial cell angiogenic responses to beta-amyloid. Exp Cell Res 312: 996–1010.
32. Chapman KE, Sinclair SE, Zhuang D, Hassid A, Desai LP, et al. (2005) Cyclic mechanical strain increases reactive oxygen species production in pulmonary epithelial cells. Am J Physiol Lung Cell Mol Physiol 289: L834–841.
33. Shelat PB, Chalimoniuk M, Wang JH, Strosznajder JB, Lee JC, et al. (2008) Amyloid beta peptide and NMDA induce ROS from NADPH oxidase and AA release from cytosolic phospholipase A2 in cortical neurons. J Neurochem 106: 45–55.
34. Selkoe DJ (2001) Clearing the brain's amyloid cobwebs. Neuron 32: 177–180.
35. Iijima-Ando K, Hearn SA, Granger L, Shenton C, Gatt A, et al. (2008) Overexpression of neprilysin reduces alzheimer amyloid-beta42 (Abeta42)-induced neuron loss and intraneuronal Abeta42 deposits but causes a reduction in cAMP-responsive element-binding protein-mediated transcription, age-dependent axon pathology, and premature death in Drosophila. J Biol Chem 283: 19066–19076.
36. Turner AJ, Isaac RE, Coates D (2001) The neprilysin (NEP) family of zinc metalloendopeptidases: genomics and function. Bioessays 23: 261–269.
37. Saavedra L, Mohamed A, Ma V, Kar S, de Chaves EP (2007) Internalization of beta-amyloid peptide by primary neurons in the absence of apolipoprotein E. J Biol Chem 282: 35722–35732.
38. Lustbader JW, Cirilli M, Lin C, Xu HW, Takuma K, et al. (2004) ABAD directly links Abeta to mitochondrial toxicity in Alzheimer's disease. Science 304: 448–452.
39. Yao J, Du H, Yan S, Fang F, Wang C, et al. (2011) Inhibition of amyloid-beta (Abeta) peptide-binding alcohol dehydrogenase-Abeta interaction reduces Abeta accumulation and improves mitochondrial function in a mouse model of Alzheimer's disease. J Neurosci 31: 2313–2320.
40. Stine WB, Jr., Dahlgren KN, Krafft GA, LaDu MJ (2003) In vitro characterization of conditions for amyloid-beta peptide oligomerization and fibrillogenesis. J Biol Chem 278: 11612–11622.
41. Kim KS, Miller DL, Sapienza VJ, Chen CMJ, Bai C, et al. (1988) Production and characterization of monoclonal antibodies reactive to synthetic cerebrovascular amyloid peptide. Neuroscience Research Communications 2: 121–130.
42. Wyttenbach A, Sauvageot O, Carmichael J, Diaz-Latoud C, Arrigo AP, et al. (2002) Heat shock protein 27 prevents cellular polyglutamine toxicity and suppresses the increase of reactive oxygen species caused by huntingtin. Hum Mol Genet 11: 1137–1151.
43. Sellamuthu S, Shin BH, Han HE, Park SM, Oh HJ, et al. (2011) An engineered viral protease exhibiting substrate specificity for a polyglutamine stretch prevents polyglutamine-induced neuronal cell death. PLoS One 6: e22554.
44. Jungbauer LM, Yu C, Laxton KJ, LaDu MJ (2009) Preparation of fluorescently-labeled amyloid-beta peptide assemblies: the effect of fluorophore conjugation on structure and function. J Mol Recognit 22: 403–413.